Shrinkage Cracking in Physical Model of Undisturbed Expansive Clay Slope subjected to Wet-Dry Cycles

A.C. Amenuvor, G-W. Li*, Y-Z. Hou & W. Chen

Key Laboratory of Ministry of Education for Geomechanics and Embankment Engineering, Hohai University, Nanjing, China
**Highway and Railway Research Institute, Hohai University, Nanjing, China*

ABSTRACT: The strength and stability of expansive soil slopes is strongly influenced by shrinkage cracking resulting from multiple wet-dry cycles. This study investigates the structural and crack development in a physical model of undisturbed expansive clay slope under five of wet-dry cycles. The model is 150 cm long, 80 cm wide and 80 cm high, and has slope inclination of 1:1.7. The surface distribution of crack networks was monitored with a digital camera and the images obtained were analysed using image processing technique to quantify the surface crack parameters in terms of crack intensity factor (CIF). The CIF increased and stabilize at 15% in the third cycle. CIF also increased linearly with decreasing water content to stabilize at water content of 9%. Changes in suction occurred to a depth of 28 cm, and the maximum suction increased with increasing cycle number. Vertical cracks whose bases are connected by near horizontal cracks or cracks parallel to the slope developed to a maximum depth of 28 cm.

1 INTRODUCTION

Expansive soils undergo desiccation cracking when subjected to water loss. The presence of expansive minerals in expansive clays causes these soils to shrink and swell in response to seasonal fluctuations in water content. Swelling/shrinkage resulting from wetting/drying of expansive soils causes the soil to undergo significant structural changes resulting in changes in soil behaviour. The development and extent of desiccation cracks is influenced by several factors including clay content and mineralogy, soil thickness, rate of drying, total drying time etc. (Colina and Roux 2000; Nahlawi and Kodikara 2006; Fang and Chaney 2016)

The cracks create zones of weakness in a soil mass and cause reduction in the overall strength and stability. Cracks also have significant influence on the rate of infiltration and permeability of the soil mass. The hydraulic properties of the soil are directly controlled by the crack networks (Chertkov 2000). The development of desiccation cracks in slopes can have significant impact on the stability of the slopes. The cracks provide preferential flow path which can increase the soil hydraulic conductivity and decrease the soil strength as a result of decreased matric suction when the soil is wet. Also, water in cracks can increase the weight of the soil mass and exert an additional driving force on the slope. In addition, cracks can form a part of the critical slip surface.

The number of wet-dry cycles a soil undergoes also affects the development of cracks and hence the structure (Hussein and Adey 1995) and mechanical behaviour of the soil. Yesiller et al. 2000 observed that the amount of cracking did not vary much after the second cycle. Several studies have indicated that the shear strength parameters of expansive soils reduce under multiple cycles of drying and wetting (Goh et al. 2013, Hossain et al. 2016).

Numerous research has been dedicated to studying the desiccation cracking of expansive soils under wet-dry cycles. A vast amount of these studies have been conducted on small-sized undisturbed, compacted soil or slurry soil specimens in the laboratory (e.g. Goehring et al. 2010, Atique and Sanchez, 2011, Tang et al. 2011). A few of these studies, however, involved scaled model tests on compacted expansive soils (Miller 1998, Yesiller et al. 2000). The study presented here investigates the development of cracks in a physical model of undisturbed expansive clay slope subjected to five wet-dry cycles. The model soil was extracted from the Yangtze river - Huai river canal construction experimental project site.

2 MATERIALS AND METHODS

2.1 *Model tank and soil extraction*

The model facility consists of a rigid steel tank with inner dimensions of 150 cm long, 100 cm width and

100 cm deep. In order to extract the soil undisturbed, the model tank was designed to be portable, with plates and rigid frame components that could easily be assembled around the soil. It consists of four 5 mm thick steel side plates, a 5 mm thick bottom steel plate and rigid steel frames at all four sides, which could be assembled and connected with bolts and nuts. Two 20 mm thick glass boards were used to replace the steel plates at two of the longest sides after soil extraction and transportation.

The soil used in the experiment was extracted from the Yangtze river - Huai river canal construction project site from a depth 7 m below the surface. In order to extract the soil with minimal soil disturbance, a 3 m x 2 m area containing the soil of interest was first marked out. An excavator was then used to carefully to dig the material around this area to a depth of 2 m, leaving an isolated 12 m^3 of intact clay. This isolated volume of soil was then carefully trimmed down, to the desired 1.5 m x 1 m x 1 m size to fit into the model tank. Figure 1 shows the soil extraction process.

Figure 1. Soil extraction in the field: (a) trimmed soil; (b) trimmed soil in model tank

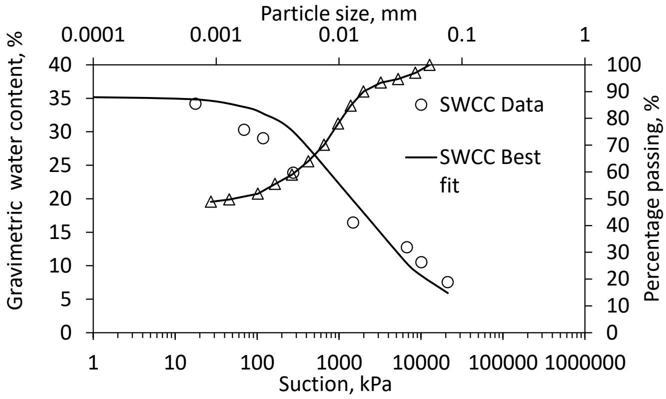

Figure 2. Soil water characteristics curve and particle distribution curve of the soil

2.2 *Soil type and index properties*

The soil used is classified as CI according to the unified soil classification system. The index properties and mineralogical composition of the soil are presented in Table 1. The soil water characteristics curve, which was determined using the filter paper method, and the particle size distribution curve for the soil are shown in Figure 2.

Table 1. Summary of measured soil properties

Property	
Mineralogical composition	
Quartz (%)	55
Feldspar (%)	21
Montmorillonite (%)	12
Mica (%)	4
Kaolinite	4
Chlorite	3
Vermiculite	1
Specific gravity	2.72
Free swell index (%)	70
Atterberg limits	
Plastic limit (%)	13
Liquid limit (%)	47
Plasticity index (%)	34
Unified soil classification system (USCS)	CI

2.3 *Slope Preparation and Experimental Setup*

Upon transporting the model tank with the soil to the experiment site, the side steel plates of the longest sides were replaced with the glass boards after the sides were trimmed down to the desired 80 cm width. The slope was then carefully excavated with trowel and spade, which were well sharpened to avoid disturbance to the soil and obtain very smooth initial soil surface for analysis of cracks. The excavated slope was 150 cm long, with crest height of 80 cm and toe height of 35 cm. The length of the crest and the toe are 40 cm and 35 cm, respectively. And the slope inclination is 1:1.7.

Suction and water content measurements were made using heat dissipation matric potential sensors and soil moisture sensors installed at various depths within the soil. Figure 3(a) shows a schematic of the model instrumentation. To avoid disturbance to the surface of the surface, the sensors were installed in horizontal holes drilled on one of the sides of the slope before placement of the glass board.

A digital camera was fixed on top of the model tank to take periodic photographs of the sloping surface for performing image analysis of cracks developed during various wet/dry cycles. The drying was carried out using a heater with a blower positioned in the tank, near the toe of the slope. Wetting was induced by an oscillating nozzle which sprayed water uniformly on the surface of the soil. Figure 3(b) shows the experimental setup. Water was allowed to run out of the model through holes in the model tank, near the toe of the slope.

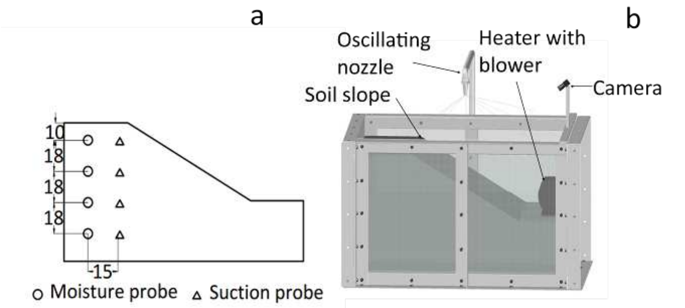

Figure 3. Instrumentation and experimental setup: (a) instrumentation; (b) experimental setup

2.4 *Drying and wetting cycles*

The model slope was subjected to alternate wet-dry cycles, during which period water content, matric suction readings were taken daily. In addition to water content measurement by the soil moisture sensors, soil samples were taken near the soil surface for determination of gravimetric water content at various drying stages of the experiment. Photographs of the surface of the soil were taken at certain intervals during each drying phase to capture the development of desiccation cracks

Drying in each cycle was induced by a rotating heater equipped with a blower to ensure good circulation of heat, while at the same time simulating wind action. The temperature and relative humidity in the tank varied between 18 to 35°C and 65 to 80%, respectively. Drying process was terminated when crack conditions on the soil surface stabilized. Rainfall with intensity of 30 mm/h was applied to the surface of the soil at the end of each drying cycle. The rainfall application was terminated when suction measured by the two top most sensors reduces to around 10 kPa.

3 RESULTS AND DISCUSSIONS

3.1 *Visual observations*

In as little as 30 minutes to an hour into the drying phase numerous tiny polygonal cracks developed simultaneously, covering the entire soil surface. However, most of these cracks were barely visible until about an hour and half into drying when the cracks became obvious as hair-like polygons (Figure 4a). With progression of time into the drying phase, some of the cracks widened and deepened, particularly near the crest of the slope (left of side of Figure 4b). At the end of the drying phase, up to 1.0 cm wide cracks were observed, mostly near the crest of the slope.

The wetting event after the first drying phase resulted in complete closure of all cracks on the surface of the soil in less 30 minutes of wetting, with the water content reaching 49% at the crest of the slope. The wetting event also caused erosion on the surface of the soil, despite covering the surface of the soil with geotextile.

During the second drying phase, linear cracks only started appearing on the surface of the soil in about 27 hours of drying. This could be attributed to the high water content of the soil. Again, unlike the first cycle, the second cycle started with the appearance of linear cracks. As time progressed, more and more cracks appeared mainly at their original locations. The cracks in the second cycle are much deeper and wider than the first cycle. Also, unlike the first cycle, the cracks in the second cycle have more uniform width with average width of 1.0 cm. A few cracks particularly near the crest of the slope attained maximum width of 1.3 cm. The second drying phase produced well-defined aggregation of soil particles.

The third, fourth and fifth cycles were similar to the second cycle with respect to the time of initiation and the rate of development of surface cracks. However, the width of cracks in the latter cycles was larger and more uniform than the previous cycles. Besides a few isolated cracks with width of 2.5 cm at the cracks, most of the cracks covering the surface of the slope have average width of 1.3 cm. In addition, the pattern of cracks in the third, fourth and fifth cycles are almost identical and different from those in the first and second cycles, indicating equilibrium in surface crack development in the third cycle. Figure 5a and Figure 5b shows the surface cracks at the end of the second and fifth cycles, respectively.

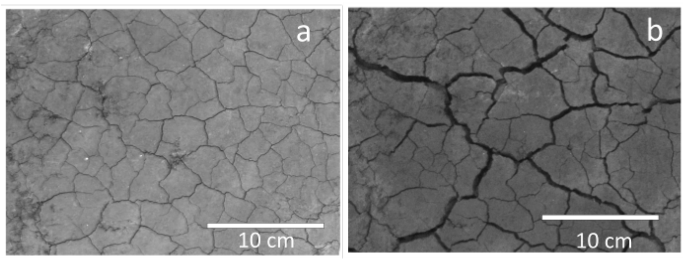

Figure 4. Crack evolution during the first drying phase: (a) surface cracks 1 and half hour of drying; (b) surface cracks at the end of drying

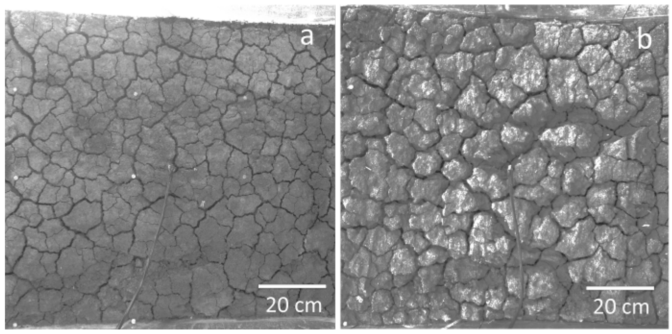

Figure 5. Evolution of surface cracks at the end of various drying cycles: (a) second cycle; (b) fifth cycle

As mentioned earlier, the wetting event after the first drying resulted in complete disappearance of the surface cracks (Figure 6a). The complete disappearance of cracks during the first wetting event may be due to the total collapse of particle aggregates because of particle separation. The changes that occur can lead to the instability of some structural units due to softening of aggregates and the breakage of particle contact bonds (Wilding and Puentes 1988). In the wetting events of the following cycles, however, some of the major surface cracks persisted, indicating that some of the structural changes in the soil are irreversible. More and more surface cracks persisted during successive wetting events as the number of wet-dry cycles increased. Figure 6b shows the soil surface after the fifth wetting, with some cracks and erosion patterns. It had been observed that if the soil mass has previously undergone drying, then additional bonding will be generated between the particle contacts resulting in stiffening of aggregates, which resists the total failure of the developed structure. This process is considered to be analogous to the pre-consolidation soil experiences through drying and subsequent unloading, which results in a more stable structure (Mitchell and Soga 2005). This may be the reason for the persistence of surface cracks during wetting in the latter cycles.

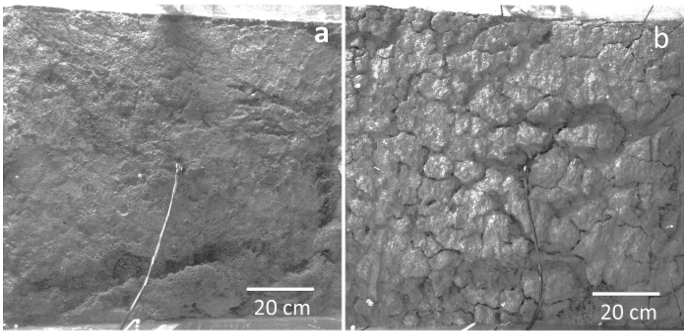

Figure 6. Soil surface morphology after wetting: (a) first cycle; (b) fifth cycle

3.2 *Suction and water content*

Measurements from the soil moisture probes were unrealistically too low or unstable and therefore are not presented here.

Figure 7 presents changes in suction during the various wet/dry cycles. Figure 7 shows a more rapid increase in suction at 10 cm depth compared to 28 cm depth as the rate of desiccation is much faster near the surface and slows down with increasing depth. The decrease in suction during wetting is however dramatic at both 10 cm and 28 cm depths, though it was a bit slower for the 28 cm depth. As the intensity of cracking gets lower with depth, the soil permeability correspondingly decreases with depth resulting in slower decrease in suction during wetting. The peaks in Figure 7, which shows increasingly higher suction with increasing wet/dry cycle, correspond to the suction at the end of each cycle. As the upper limit for reliable suction measurement by the sensors used is 2500 kPa, suction values in the figure are truncated at 2500 kPa. Generally, increasingly higher suctions with increasing wet/dry cycle number were also obtained at the depth of 28 cm. An exception to the increasingly higher suction with increasing cycle number occurs in the fourth and fifth cycles. As seen in Figure 7, the period of fourth drying cycle was extended, and this resulted in significantly higher suction of 473 kPa than the other cycles at the depth of 28 cm. For the same reason, a plateau in suction occurs in the fourth cycle at the 10 cm depth in Figure 7. No change in suction was measured at the depths of 46 cm 64 cm, so no data is presented on these depths. Under repeated wet-dry cycles, many soils tend to develop stable structure due to rearrangement of soil particles to achieve potential energy minima (Quirk and Murray, 1991). This involves aggregation of soil particles to form a stiffer structure (Dalrymple and Jim, 1984; Wilding and Puentes, 1988). A stiffer structure means packing of soil particles closer together and hence smaller pore sizes, and higher suctions are expected to develop in soils with small pore sizes. The observed increasingly higher suction with increasing number of wet/dry cycles may be attributed to development of stable and stiffer structure leading to reduced pore sizes as the number of wet/dry cycles increased. It should however be noted that the soil again becomes weak when wet.

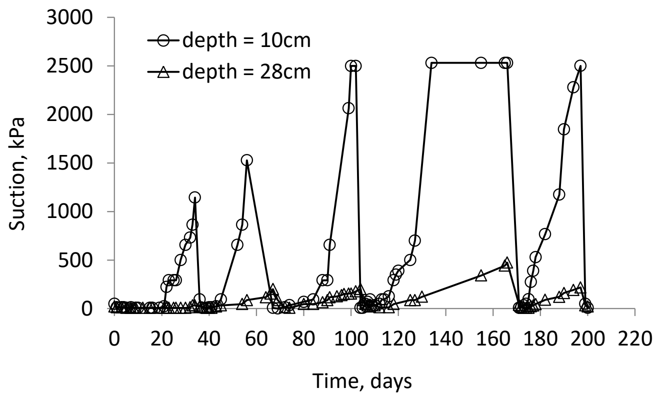

Figure 7. Variation of suction over various wet/dry cycles

3.3 *Crack development at depth*

Two sets of vertical cracks were observed, through the glass boards, during the alternate wetting and drying cycles. The first set of cracks (coloured red in Figure 8), here referred as primary vertical cracks developed down to the depth varying from 8 cm near the toe of the slope to 13 cm at near the crest region. The spacing of these cracks corresponds to the spacing of the polygonal cracks on the surface. The cracks are connected at their bases by near horizontal cracks. The second set of cracks here referred to as the secondary vertical cracks developed after the first wet/dry cycle and in the later periods of each drying phase. These cracks penetrated the soil to depth varying from 10 cm near the toe of the slope to 28 cm near the crest. They began to appear in the second cycle as isolated cracks which were widely and irregularly spaced. They formed as extensions of some of the primary vertical cracks. As the number of cycles increased, their numbers increased and their spacing reduced, and they became connected at the bases by near horizontal cracks. Structural development in vertisols may result in the formation of slickensides, which occurs within from 25 cm – 1 m depth (Dudal and Eswaran 1988). Slickensides form as water passes into the bottom of the vertical cracks formed during drying, causing excess moisture at the bottom, which in turn causes swelling pressure leading to shear failure of the soil. This may explain the formation of the near horizontal cracks observed.

Photographs taken from the sides of the slope through the glass boards do not clearly show the cracks and are not presented here. A sketch of the side cracks as visually observed is, however, presented in Figure 8. The connectivity of the secondary vertical cracks at their bases makes the base these cracks a weak zone along which sliding, or failure may occur. The persistence of the vertical cracks along the entire span of the slope is indicative that slope failure can originate from anywhere along the slope. The depth and orientation of cracks in Figure 8 may explain the commonly observed phenomenon of shallow slope failure in clays. The slip surface and its depth would be controlled by the depth of secondary vertical cracks and the near horizontal cracks at their bases.

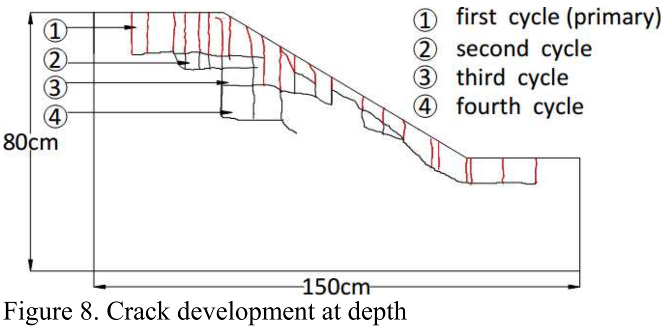

Figure 8. Crack development at depth

3.4 *CIF and water content variation with time and cycle number*

The extent of cracking at the surface of the soil is quantified by using the crack intensity factor (CIF), a method introduced by Miller (1998). The crack intensity factor is defined as the area of cracks divided by the total surface area of soil. Photographs of the cracking surface were processed by image analysis technique to determine the area covered by cracks, through computing the area of pixels covered by the cracks, which was then divided by the surface area of the soil to determine the CIF. The image processing leading to determination of CIF basically entails converting the original coloured (RGB) image to grey scale image (Figure 9a) which in turn is converted to binary image (Figure 9b). The ratio of white pixels to black pixels in percentage is the CIF.

During each drying phase, the water content at the surface within the zone of drying was measured periodically by gravimetric method. Figure 10 shows how CIF and water content varied with time during the first drying phase. The rate of development of cracks is closely related to the rate of desaturation of the soil. This is evident in the fact that the water content and CIF curves form mirror image of each other as seen in Figure 10. CIF increased as water content decreased and the slope of the two curves are very similar throughout the entire drying phase. In Figure 10, notable desiccation cracking was observed just one hour into the drying phase with the CIF increasing sharply to 5.7% at water content of 23%. The CIF then increased sharply to 10.5% with correspondingly sharp decrease in water content to 10.2% six hours into the drying phase. Thereafter, the CIF increased gently to 11.8% in 72 hours after which it stabilized. At the same time, the water content decreased gradually and stabilized around 9%.

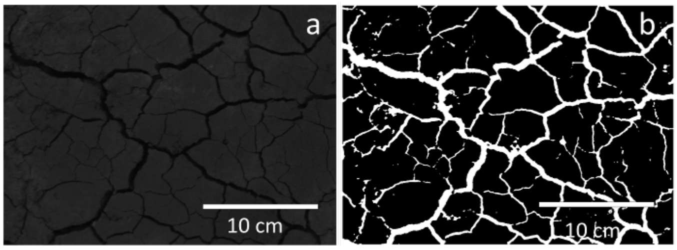

Figure 9. Image analysis process: (a) grey scale image; (b) binary image

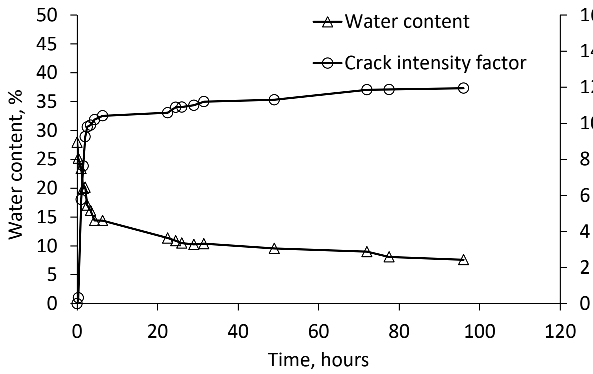

Figure 10. Change in water content and CIF with time in the first cycle

Figure 11 shows a plot of CIF as a function of cycle number. Very notable is the high number of cracks developed in the first cycle, indicated by the high CIF of 12.3%. Crack development stabilized in the third cycle with CIF of 15.5%. The increased in CIF after the first cycle did not result from the development of new cracks in subsequent cycles, but rather because of widening of some of the cracks developed earlier. Figure 12 shows the relation between crack intensity factor and surface water content for the first and second cycles. The crack intensity factor increased linearly with decreasing water content and then ceased to increase around a water content of 9%. The difference in slope of the curves is due to dramatic increase in water content during wetting after the first drying because of significant cracking and structural changes in the soil.

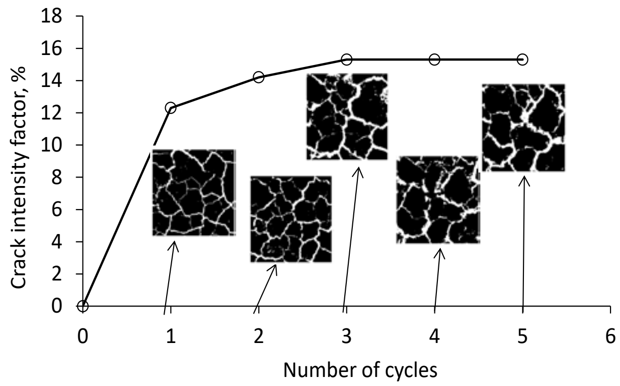

Figure 11. Variation of CIF with number of dry/wet cycle

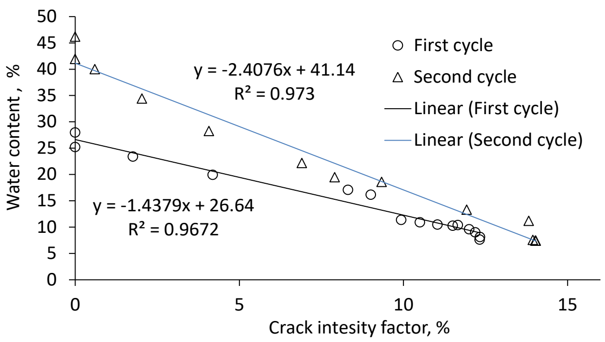

Figure 12. Variation of crack intensity factor with water content for first cycle

4 CONCLUSIONS

This study investigated the development of cracks in a substantial physical model of an undisturbed expansive clay slope subjected to five cycles of wetting and drying. The findings of the study are summarized herein.

Significant cracking occurred in the soil in the first wet-dry cycle resulting in crack intensity factor (CIF) of 12.3%. The CIF stabilized around 15% in the third cycle. Some of the cracks developed in the first cycle were healed after wetting and did not reappear in subsequent cycles. The increase in CIF in subsequent cycles was due to increase in the width of cracks rather than increase in the number of cracks. The CIF increased linearly with decreasing water content, and then ceased to increase any further when the water content reached 9%.

Changes in suction occurred down to a depth of 28 cm in each wet-dry cycle, with suctions measured 10 cm below the soil surface significantly higher than at 28 cm depth. The rate of increase and decrease in suction during drying and wetting, respectively, was faster at shallower depths. The maximum suction attained in each cycle increased with increasing number of wet-dry cycles.

Near vertical cracks developed in the soil along the entire span of the slope reaching a depth of 28 cm. These vertical cracks are connected at their bases by near horizontal cracks or cracks parallel to the surface of the slope.

5 REFERENCES

Atique, A. & Sanchez, M. 2011. Analysis of Cracking Behavior of Drying Soil. *Proceedings of the 2nd International Conference on Environmental Science and Technology IPCBEE, Singapore* 6: 66-70

Chertkov, V.Y. 2000. Using Surface Crack Spacing to Predict Crack Network Geometry in Swelling Soils. *Soil Science Society of America Journal* 64(6): 1918-1921.

Chertkov, V.Y. & Ravina, I. 1999. Tortuosity of Crack Networks in Swelling Clay Soils. *Soil Science Society of America Journal* 63(6): 1523-1530.

Colina, H. & Roux, S. 2000. Experimental Model of Cracking Induced by Drying Shrinkage. *The European Physical Journal E: Soft Matter and Biological Physics* 1(2): 189-194.

Dalrymple, J.B. & Jim, C.Y. 1984. Experimental Study of Soil Microfabrics Induced by Isotropic Stresses of Wetting and Drying. *Geoderma* 34(1): 43-68.

Dudal, R. & Eswaran, H. 1988. Distribution, Properties and Classification of Vertisols. *Vertisols: Their Distribution, Properties, and Management (Wilding L.P., & Puentes R.) Texas A&M Press: College Station, TX;* 1-22.

Fang, H.Y. & Chaney, R.C. 2016. *Introduction to Environmental Geotechnology*. CRC press. 161 pp.

Goehring, L., Conroy, R., Akhter, A., Clegg, W.J. & Routh, A.F. 2010. Evolution of Mud-Crack Patterns during Repeated Drying Cycles. *Soft Matter* 6(15): 3562–3567.

Goh, S.G., Rahardjo, H.E. & Leong, E.C. 2013. Shear Strength of Unsaturated Soils under Multiple Drying-Wetting Cycles. *Journal of Geotechnical and Geoenvironmental Engineering*, ASCE 140(2): 6013001.

Hossain, S., Kong L-W. & Yin, S. 2016. Effect of Drying-Wetting Cycles on Saturated Shear Strength of Undisturbed Residual Soils. *American Journal of Civil Engineering* 4(4): 143-150.

Hussein, J. & Adey, M.A. 1995. Changes of Structure and Tilth Mellowing in a Vertisol due to Wet/dry Cycles in the Liquid and Vapour Phases. *European Journal of Soil Science* 46(3): 357-368.

Miller, C.J. 1998. Experimental Analysis of Desiccation Crack Propagation in Clay Liners. *Journal of American Water Resources Association*, AWRA 34(3): 677-686.

Mitchell, J.K. 1993. *Fundamentals of Soil Behavior*. John Wiley & Sons.

Nahlawi, H. & Kodikara, J.K. 2006. Laboratory Experiments on Desiccation Cracking of Thin Soil Layers. *Geotechnical and Geological Engineering* 24(6): 1641-1664.

Quirk, J.P. & Murray, R.S. 1991. Towards a Model for Soil Structural Behavior. *Soil Research* 29(6): 829-867.

Tang, C-S., Cui, Y-J., Shi, B., Tang, A-M. & Liu, C. 2011. Desiccation and Cracking Behaviour of Clay Layer from Slurry State under Wetting--Drying Cycles. *Geoderma* 166(1): 111-118.

Yesiller, N., Miller, C.J., Inci, G., & Yaldo, K. 2000. Desiccation and Cracking Behavior of Three Compacted Landfill Liner Soils. *Engineering Geology* 57(1): 105-121.